Biomaterials Science

ROYAL SOCIETY OF CHEMISTRY

PAPER

View Article Online
View Journal | View Issue

Cite this: *Biomater. Sci.*, 2024, **12**, 5253

Crosslinked hybrid polymer/ceramic composite coatings for the controlled release of clindamycin

Dagmara Słota, *[a] Mateusz M. Urbaniak, [b,c] Agata Tomaszewska,[b,d] Karina Niziołek,[a] Marcin Włodarczyk,[b] Wioletta Florkiewicz,[e] Aleksandra Szwed-Georgiou, [b] Agnieszka Krupa[b] and Agnieszka Sobczak-Kupiec[e]

A major risk associated with surgery, including bone tissue procedures, is surgical site infection. It is one of the most common as well as the most serious complications of modern surgery. A helpful countermeasure against infection is antibiotic therapy. In the present study, a methodology has been developed to obtain clindamycin-modified polymer–ceramic hybrid composite coatings for potential use in bone regenerative therapy. The coatings were prepared using a UV-light photocrosslinking method, and the drug was bound to a polymeric and/or ceramic phase. The sorption capacity of the materials in PBS was evaluated by determining the swelling ability and equilibrium swelling. The influence of the presence of ceramics on the amount of liquid bound was demonstrated. The results were correlated with the rate of drug release measured by high-performance liquid chromatography (HPLC). Coatings with higher sorption capacity released the drug more rapidly. Scanning electron microscopy (SEM) imaging was carried out comparing the surface area of the coatings before and after immersion in PBS, and the proportions of the various elements were also determined using the EDS technique. Changes in surface waviness were observed, and chlorine ions were also determined in the samples before incubation. This proves the presence of the drug in the material. The *in vitro* tests conducted indicated the release of the drug from the biomaterials. The antimicrobial efficacy of the coatings was tested against *Staphylococcus aureus*. The most promising material was tested for cytocompatibility (MTT reduction assay) against the mouse fibroblast cell line L929 as well as human osteoblast cells hFOB. It was demonstrated that the coating did not exhibit cytotoxicity. Overall, the results signaled the potential use of the developed polymer–ceramic hybrid coatings as drug carriers for the controlled delivery of clindamycin in bone applications. The studies conducted were the basis for directing samples for further *in vivo* experiments determining clinical efficacy.

Received 11th January 2024,
Accepted 24th July 2024

DOI: 10.1039/d4bm00055b

rsc.li/biomaterials-science

Introduction

In 2019, the number of new cases of bone fractures as well as injuries worldwide was estimated as 178 million, which represents an increase of 33.4% since 1990. Approximately 7% of fractures required surgical intervention and implantation of biomaterials to fill structural defects and/or restore bone tissue function. The increase in the incidence of bone injuries due to the emergence of lifestyle diseases, *i.e.* osteoporosis, has contributed to the increased investment in the development and implementation of new biomaterials. According to a report prepared by Vantage Market Research, the global market for biocomposites used in regenerative medicine was valued at $24.2 billion in 2021 and is expected to reach about $57.5 billion by 2028 at a CAGR of 15.5%.[1,2] Key factors driving this market are the increasing number of road traffic accidents, the rising incidence of acquired or congenital deformities, and technological advances in plastic surgery.[3,4]

Nowadays, a lot of attention is being given to the development of multifunctional materials, whose purpose will be not only to fill the defect, but also to provide the implant with other functions, such as being a carrier of an active substance or a drug.[5] The release of the drug at a specific lesion site can

[a]*Cracow University of Technology, CUT Doctoral School, Faculty of Materials Engineering and Physics, Department of Materials Engineering, 37 Jana Pawła II Av., 31 864 Kraków, Poland. E-mail: dagmara.slota@pk.edu.pl*
[b]*University of Lodz, Faculty of Biology and Environmental Protection, Department of Immunology and Infectious Biology, 12/16 Banacha St, 90-237 Łódź, Poland*
[c]*University of Lodz, Faculty of Chemistry, Department of Inorganic and Analytical Chemistry, 12 Tamka St, 91-403 Łódź, Poland*
[d]*Bio-Med-Chem Doctoral School of the University of Lodz and Lodz Institutes of the Polish Academy of Sciences, 12/16 Banacha St, 90-237 Łódź, Poland*
[e]*Cracow University of Technology, Faculty of Materials Engineering and Physics, Department of Materials Engineering, 37 Jana Pawła II Av., 31 864 Kraków, Poland*

effectively accelerate tissue regeneration and patient recovery.[6] This is highly important in terms of surgical site infections (SSI), such as those after bone grafts. SSI are the most common infections that can occur both during hospitalisation as well as after hospital discharge.[7] The etiologic agent leading to infections is most often bacteria residing on the skin, but can also be microorganisms residing in other areas of the body or found in the operating room environment, as well as on surgical instruments.[8] Bacterial infections are highly dangerous as they can lead to osteomyelitis, which is defined as an inflammatory process caused by a bone infection that leads to bone destruction and bone necrosis, and eventually can progress to a chronic condition.[9,10] According to the procedure recommended by the World Health Organization, antibiotic therapy can effectively prevent infection.[11] Therefore, the development of a biomaterial that is capable of releasing the drug directly at the site requiring a therapeutic effect and protection is a real opportunity to improve the health of patients.

The work presented here involves the development of hybrid composite coatings based on synthetic polymers like poly(vinylpyrrolidone) (PVP), poly(ethylene glycol) (PEG) and poly(ethylene glycol) diacrylate (PEGDA) as well as natural ones like collagen (COL). PEG especially in a hydrogel form is a well-known flexible biomaterial approved by the Food and Drug Administration (FDA), USA, for various biomedical uses. It is characterised by exceptional tunability and biocompatibility, and its softness as well as elasticity make it similar to natural tissues. Chemically, this polymer is composed of a repeating subunit of ethylene glycol ($HO–CH_2–CH_2–OH$), and its structure can be described as $H–(O–CH_2–CH_2)_n–OH$.[12,13]

Similar biological properties are demonstrated by PVP, which is biocompatible and biodegradable and has good water solubility. It also has one of the lowest cytotoxicities among synthetic polymers.[14,15] Similar to PEG, it has been approved by the FDA, USA for a wide range of applications. Commercially, the most common uses are as hydrogels for wound dressings and binders in pharmaceuticals.[16] It consists of a repeating *N*-vinylpyrrolidone monomer, and its mer structure can be expressed as $–[CH_2CH(C_4H_6NO)]–$.[17]

However, in the aspect of bone regeneration, it is COL that has the most significant properties, as it is a protein biopolymer that occurs in large quantities in the connective tissues of animal organisms, including humans. It is the main structural component of skin, bones, tendons, ligaments and other tissues, as well as being the principal ingredient in the extracellular matrix. COL is applied in bone regeneration to provide structural support, stimulate bone cell growth and restore natural bone tissue.[18,19] A typical structural element of COL is a triple helical rod-like domain composed of three polypeptide chains of glycine, proline and hydroxyproline.[20,21] So far, 29 different types of collagen have been discovered, which differ in their molecular isoforms. Most commonly used in biomedical applications are types I, II and III.[22]

Besides the aforementioned polymers, furthermore, the entire coating's structure has been enriched with glutathione (GSH) and hydroxyapatite (HAp) to increase the biological value. Glutathione is a tripeptide composed of the amino acid residues of glutamic acid, cysteine and glycine and it exhibits antioxidant properties that are manifested in the restoration of thiol (–SH) groups in proteins. It is also considered as an inhibitor of the inflammatory response involving reactive oxygen species (ROS). ROS play a significant role in the metabolism and ageing of living organisms due to the presence of an O–O bond or an oxygen atom with an unpaired electron. Reducing ROS-induced oxidative stress damage has been proved to be possible with the presence of GSH, which enhances metabolic detoxification. This tripeptide is found in all plant and animal organisms, and with age, its amount decreases.[23–25]

In this work, physicochemical as well as biological analyses were performed to determine the potential for using the developed hybrid ceramic/polymer coatings as a clindamycin carrier for targeted therapy. Such a therapy enables the drug to be released directly at the lesion site requiring a therapeutic effect. Moreover, it allows an appropriate dose of the substance to be tailored to the individual patient's needs. The study provides the basis for directing biomaterials for further *in vivo* analyses.

Materials and methods

Materials

Synthetic and natural polymers as well as the other components necessary for the synthesis of the polymer matrix, *i.e.*, polyvinylpyrrolidone (PVP), polyethylene glycol (PEG), poly (ethylene glycol) diacrylate Mn 575 (PEGDA), 2-hydroxy-2-methylpropiophenone (97%), peptide L-glutathione (reduced 98%) (GSH) and collagen from bovine Achilles tendon (COL), were purchased from Sigma-Aldrich (Darmstadt, Germany). All reagents used for hydroxyapatite (HAp) syntheses, *i.e.*, calcium acetate monohydrate ($Ca(CH_3CO_2)_2{\cdot}H_2O$), sodium phosphate (dibasic) (Na_2HPO_4), and ammonia water (NH_4OH, 25%), were also obtained from Sigma-Aldrich (Darmstadt, Germany). The measurement of sorption capacity was carried out in a Phosphate Buffered Saline (PBS) solution prepared from tablets (Oxoid, United Kingdom). Clindamycin hydrochloride was the active ingredient selected for coating modification and was purchased from Sigma-Aldrich (Darmstadt, Germany). Drug release was determined by high-performance liquid chromatography (HPLC), where the mobile phase was a combination of acetonitrile from Honeywell (Seelze, Germany) and KH_2PO_4 from DOR-CHEM (Krakow, Poland).

Bacterial strain and cell lines used in biological studies. *Staphylococcus aureus* (*S. aureus*) ATCC 29213, the L929 (CCL-1™) cell line of mouse fibroblasts and the hFOB 1.19 (CRL-3602™) cell line of human fetal osteoblasts were purchased from ATCC (Manassas, VA, USA). Cell culture media RPMI-1640 and DMEM/Nutrient Mixture F-12 Ham were bought from Sigma-Aldrich (Darmstadt, Germany), fetal bovine serum (FBS) were bought from Cytogen (Lodz, Poland), antibiotics added to cell cultures (penicillin and streptomycin)

were purchased from Biowest (Nuaillé, France) and geneticin was bought from Gibco (Waltham, MA, USA). Resazurin and 3-(4,5-dimethylthiazol-2-yl)-2,5-diphenyltetrazolium bromide (MTT) were obtained from Sigma-Aldrich (Darmstadt, Germany). ELISA kits for detecting rat IL-1β, IL-10, and TNF-α were purchased from R&D Systems (Minneapolis, MN, USA).

Material preparation

Hydroxyapatite and composite coatings were prepared as previously described.[26] This work is a continuation of the research efforts on developing drug carriers. Based on previous studies on the modification of ceramic powders with clindamycin, the powder described in an earlier publication as C/s-1.67 was selected.[27]

Polymer and composite coatings based on PVP, PEG with collagen and glutathione enriched with HAp were prepared, according to the composition presented in Table 1. In order to carry out the photocrosslinking reaction under UV light, a photoinitiator, 2-hydroxy 2-methylpropiophenone, and a crosslinking agent in the form of poly(ethylene glycol) diacrylate (PEGDA) average Mn 575 were also added.

A–C coatings were modified with clindamycin by combining the drug with a polymeric and/or ceramic phase. 5 carriers were obtained, as presented in Table 2. To modify the polymer phase with the drug, a solution containing 30 mg of clindamycin was prepared. Next, appropriate amounts of PVP and PEG polymers were dissolved in the drug solution to obtain a concentration of 15%. In the next step, GSH, PEGDA and a photoinitiator were added, and the whole mixture was subjected to photocrosslinking under UV light. The steps were repeated for coatings 2 and 4, considering the respective amounts of COL and HAp. Coatings 3 and 5 contained clindamycin-enriched HAp, which was modified as described earlier.[27]

Schematically, the composition of the coating materials and the synthesis conditions as well as a picture of an example of a finished coating applied to a PLA plate are presented in Fig. 1.

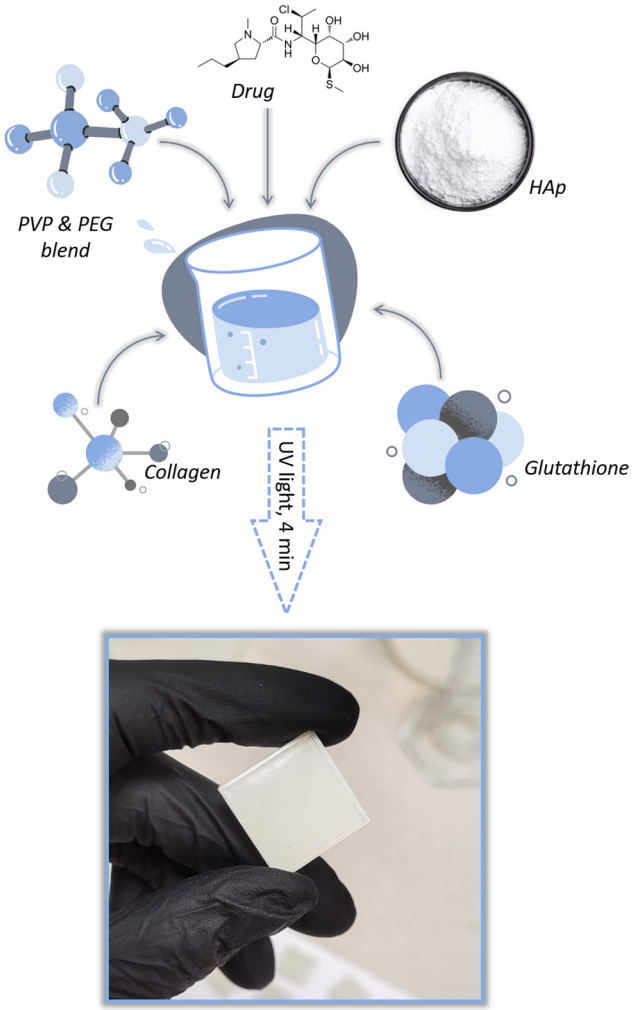

Fig. 1 Schematic of the coating material composition, the synthesis conditions and a picture of an example of a finished coating applied to a PLA plate.

Table 1 Coating composition

Coating symbol	PVP 15% [mL]	PEG 15% [mL]	GSH [g]	COL [g]	HAp [% w/v]
A	5	5	2	—	—
B	5	5	2	0.04	—
C	5	5	2	0.04	5
D	5	5	2	0.04	15

Table 2 Composition of the developed composite and polymeric clindamycin carriers

Coating symbol	Composition
1	Coating A with the drug in a polymer matrix
2	Coating B with the drug in a polymer matrix
3	Coating C with drug-modified HAp
4	Coating C with the drug in a polymer matrix
5	Coating C with drug-modified HAp and with the drug in a polymer matrix

Determination of sorption capacity

The composition of materials can affect both their structure and their swelling ability, which is understood as the ability to absorb water and/or other liquids into the polymer structure. As a result, an increase not only in the mass but also in the volume of the material occurs.

To study the swelling capacity of composite coatings, initial samples of 1 g were prepared and immersed in 100 ml of PBS, and then weighed after a specified incubation time (15 minutes, 30 minutes, 1 h, 2 h, 1 day, 2 days, 3 days or 7 days). For this purpose, after pulling the sample from the PBS solution, the excess liquid from the surface was drained with filter paper. The incubation process of the materials was carried out at 36.6 °C. The sorption capacity of the samples was then calculated according to eqn (1), where m_0 is the mass

of the dry sample and m_1 is the mass of the sample at the specified incubation time:

$$\text{Swelling ability} = \frac{m_1 - m_0}{m_0} \times 100\%. \quad (1)$$

The kinetics of composite swelling was determined by defining equilibrium swelling and the rate parameters. For this purpose, the Voigt-based viscoelastic model (eqn (2)) was used, where S_e is the equilibrium swelling [%], S_t is the swelling at time t [%], t is time [min], and τ is a rate parameter indicating the time required for the sample to absorb 0.63 of its ultimate swelling [min].[28]

$$S_t = S_e\left[1 - e^{-\frac{t}{\tau}}\right] \quad (2)$$

Incubation studies

A stability study was carried out in a PBS solution, simulating the environment of a living organism, by measuring the pH value for a period of 40 days at 36.6 °C. In parallel, the value of electrical conductivity was monitored, which provides information on the activity of ions in the incubation medium. For the measurements, an Elmetron CX-701 multifunctional device (Zabrze, Poland) with an EPS-1 pH-metric electrode and ECF-1 conductivity sensor was used.

Surface morphology

To study the surface morphology of the clindamycin-formed coatings, studies were performed using a JEOL IT200 Scanning Electron Microscope (SEM) (JEOL Ltd, MA, USA) with an EDS system detector. A comparative analysis of the clindamycin coatings before and after incubation in PBS was performed to study the changes during the incubation process. EDS examination and elemental mapping were performed after the surface testing. Before SEM measurements, the samples were coated with a gold nanolayer using a DII-29030SCTR Smart Coater sputtering machine (JEOL Ltd, MA, USA).

Drug release rate studies

To determine the rate of drug release, clindamycin-modified biomaterials were placed in sterile, sealed containers filled with 60 mL of PBS solution. The containers were then stored in an incubator (POL-EKO, Wodzisław Śląski, Poland) at 36.6 °C. The concentration of the released drug was determined by a high-performance liquid chromatography (HPLC) technique (Shimadzu, Kyoto, Japan), using the methodology described earlier.[27] Release studies were conducted over a period of 14 days.

Sterilisation and sample preparation for biological studies

Prior to biological evaluation, all tested composites were sterilised by gamma irradiation with a dose of 25 kGy with gamma rays from a ^{60}Co source at the Institute of Applied Radiation Chemistry, Lodz University of Technology in Lodz. We used 14 mm diameter discs to evaluate the antibacterial activity of the tested coatings. Tested materials of a size equal to 1/10 of the 96-well plate well surface were used in the cytocompatibility studies.

Evaluation of the antibacterial activity

The antibacterial activity of the post-incubation supernatants from the clindamycin-modified composite coatings against *S. aureus* ATCC 29213 (American Type Culture Collection, Manassas, VA, USA) was assessed using a resazurin reduction assay.[29] The percentage of metabolically active bacteria treated with the tested post-incubation supernatants of the coatings was determined in relation to the untreated culture of *S. aureus* ATCC 29213. The clindamycin-modified coatings and clindamycin-free reference samples were distributed in the wells of a 24-well plate containing 1 mL of Mueller–Hinton Broth (MHB; Sigma Aldrich, Darmstadt, Germany) and incubated for 24 h (37 °C, 5% CO_2) to obtain the post-incubation supernatants. The bacteria were cultured in MHB to a mid-log phase and the inoculum was standardised to 0.5 McFarland (5×10^5 CFU mL^{-1}) as recommended by the EUCAST guidelines.[30] The post-incubation supernatants were transferred to new wells of the 24-well plate. Then, the bacterial suspension (500 μL) was added to each well, and the plates were incubated for 24 h at 37 °C. Control wells containing the bacterial culture alone (positive control of bacterial growth) and wells with MHB alone (negative control) were included. Four independent experiments were performed in triplicate. The antibacterial activity was assessed based on the metabolic ability of the bacteria to reduce resazurin to resorufin in the milieu of the post-incubation supernatant. Prior to reading, 100 μL of 0.02% resazurin (Sigma-Aldrich, Darmstadt, Germany) in sterile PBS was added to each well and left for 3 h. Fluorescence was measured at an excitation wavelength of 560 nm and an emission wavelength of 590 nm using a SpectraMax® i3x multi-mode microplate reader (Molecular Devices, San Jose, CA, USA).

Anti-biofilm activity

S. aureus ATCC 29213 was used to evaluate the anti-biofilm activity of the tested composite coatings. The bacteria were cultured in MHB to a mid-log phase, and the inoculum was prepared at a concentration of 1×10^6 CFU ml^{-1} for the test. The clindamycin-modified coatings (1, 3, 4 and 5) and clindamycin-free reference samples (A and C) were placed in a 24-well plate, and then 1 mL of the prepared bacterial suspension was added to each well with the tested samples. The plates were incubated for one, three or seven days at 37 °C. After incubation, unbound bacteria were washed with PBS, and the formed biofilm was stained using a LIVE/DEAD™ BacLight™ kit (Thermo Fisher Scientific, Waltham, MA, USA) according to the manufacturer's protocol. After labelling, the biofilm was fixed with 80% methanol (Sigma-Aldrich, Saint Louis, MO, USA) for 15 min, and then the composite coatings were visualised using a TCS LSI Scanning Confocal Macroscope (SCM, Leica, Wetzlar, Germany).

Cytocompatibility

The composites were tested for their cytocompatibility according to the guidelines for testing components with potential

biomedical applications of The International Standard Organization (ISO-10993-5-2009) as described previously.[31,32] The research was carried out using the two cell lines: the reference line recommended by the ISO standard, mouse fibroblasts (L929), and human fetal osteoblasts (hFOB 1.19). The L929 fibroblasts were cultured in RPMI-1640 medium with 10% FBS supplemented with streptomycin (100 μg mL^{-1}) and penicillin (100 U mL^{-1}) at 37 °C and 5% CO_2 in a humidified incubator (>90% humidity). The hFOB 1.19 cell line was cultured in the DMEM/Nutrient Mixture F-12 Ham medium with the addition of 10% FBS and geneticin (0.3 mg mL^{-1}) at 34 °C with 5% CO_2 and humidity >90%. Adherent cells were detached from the culture dish using 0.25% trypsin EDTA solution. Cell suspensions at densities of 1×10^4 cells per well for L929 and 4×10^4 cells per well for hFOB 1.19 were added to the 96-well plate at a volume of 200 μL and incubated overnight under conditions appropriate for each cell line to form a monolayer. After overnight cell culture, the test materials of a size equal to 1/10 of the well surface were added to the wells with the cell monolayers. At the same time, samples containing a reference biomaterial (a medically certified peripheral venous catheter) were prepared. Cells cultured in the medium alone served as a non-treated control (NTC), while cells incubated with 0.3% H_2O_2 solution were used as a treated control (TC). The cell cultures were incubated with the test materials and the control samples for 24 h in conditions appropriate for each cell line. After incubation, the MTT (3-(4,5-dimethylthiazol-2-yl)-2,5-diphenyltetrazolium bromide) solution (5 mg mL^{-1}) was added to each well (20 μL) and incubated for 4 h. After that, the plates were centrifuged and then the supernatants were replaced with 200 μL of DMSO and mixed to dissolve the formazan crystals. The absorbance of the dissolved crystals was measured at 570 nm (Multiskan EX, Thermo Fisher Scientific, Waltham, MA, USA).

In vivo study of local tissue response and systemic response to implantation of biomaterials

The research involved using adult rats (*Rattus norvegicus*, Wistar breed) that weighed at least 220 g and were at least ten weeks old. These rats were obtained from the internal breeding facility of the Animal House of the Faculty of Biology and Environmental Protection of the University of Lodz (breeder code 048). Approval for *in vivo* experiments (42/LB 192-UZ-A/2021) was granted by the Local Animal Ethics Committee at the University of Lodz Medical School. The study included three groups with two of them containing composites (a clindamycin-free reference (C) and a modified clindamycin composite (4)) and a control group. The procedure included testing the local tissue response and the systemic response to the implantation of biomaterials. The local reaction after implantation was studied based on the PN-EN ISO 10993-6:2017 standard "Biological evaluation of medical devices/Testing of the local reaction after implantation". Since the tested composites were intended to have long-term contact with the body, observations after implantation were made at two-time points: 7 and 30 days. Briefly, 24 hours before surgery, food was withdrawn from the animals. On the day of the procedure, the skin on the rats' backs (6 × 4 cm from the angle of the scapula to the sacrum) was depilated using a shaver. During the surgical procedure, the animals were continuously anaesthetised using a mixture of isoflurane (5%) and oxygen, and the anaesthetised animals were immobilised in the abdominal position. The skin and subcutaneous tissues were incised in the midline of the spine at a length of approximately 3–4 cm, and subcutaneous pockets were created on the right and left sides of the spine. Two fragments of the same biomaterial were placed inside each pocket. Thus, each animal in the group (3 individuals per group) received two fragments of the same biomaterial (sterilised by radiation). The incised skin was sutured with single stitches and the postoperative wound was disinfected with Octenisept. To manage pain, each animal received subcutaneous injections of an analgesic drug for three consecutive days (butorphanol at a dose of 2 mg per kg body weight). After the procedure, the animals were placed individually in clean, sterile cages and their recover observed. The study involved observing the animals' behaviour (food and water intake) and general health conditions, and the healing process of postoperative wounds for 7 and 30 days.

The control group consisted of animals that had not undergone the procedure and were in good general condition, demonstrating no signs of local or systemic inflammatory reaction.

After 7 and 30 days, animals were euthanized for blood collection (to obtain the serum) and organ resection (lymph nodes, spleen, liver and kidneys).

The levels of IL-1β, IL-10, and TNF-α in the serum samples were determined using enzyme-linked immunosorbent assays (R&D Systems, Minneapolis, MN, USA) following the manufacturer's instructions.[33] The minimum detectable levels were 31.2 pg mL^{-1} for IL-1β, 62.5 pg mL^{-1} for IL-10, and 62.5 pg mL^{-1} for TNF-α. Absorbance values at 450 nm of samples and standards at serial concentrations were obtained using a Multiskan EX reader (Thermo Fisher Scientific, USA) and translated into the concentration of the evaluated biomarkers using the MyAssay Data analysis tool.

Statistical analyses

Statistical analyses and graphs for the biological studies were performed using GraphPad Prism version 9.1.0 for Windows (GraphPad Software, San Diego, CA, USA). The antibacterial activity data were compared using the Kruskal–Wallis test with Dunnett's *post hoc* test. For cytocompatibility studies and statistical analysis, the Shapiro–Wilk test was used to assess the Gaussian distribution. The Brown–Forsythe test was used to verify the equality of group variances. Data were analysed separately for each cell line using one-way ANOVA following Tukey's multiple comparison test. The Kolmogorov–Smirnov test confirmed that the *in vivo* dataset is normally distributed. Data from both within and between groups were analysed using a two-way ANOVA with Tukey's multiple comparison test. The experiments were conducted three times, with each experiment being repeated twice for technical accuracy.

A p-value of less than 0.05 was considered to be statistically significant.

Results and discussion

Polymer and composite coatings were subjected to swelling studies in order to determine their sorption capacity. The results obtained are presented in Fig. 2.

The effect of material composition on fluid binding capacity was confirmed. The smallest increment was observed for sample D, containing a 15% share of the ceramic phase, with swelling ability at 84% after 7 days in PBS. A slightly larger increase at 106% was observed for sample C, which contained a 5% share of the ceramic phase. The swelling abilities for polymer coatings A and B were significantly higher, at 117% and 124%, respectively. Thus, the sorption capacity decreased as the proportion of the ceramic phase increased. The reason for this is that the ceramic grains occupy the free spaces between the polymer chains, thus preventing fluid penetration into the material. The highest swelling ability was observed for coating B, which differed from shell A by the presence of collagen from bovine tendons. This effect is presumably caused by the properties of collagen, which has in its structure proline, an amino acid capable of binding water molecules.[34,35]

The swelling ability results are correlated with the determined equilibrium swelling (S_e), presented together with the rate (τ) parameter in Table 3. The S_e of coatings was in the range of 81.26 ± 1.63 to 108.97 ± 4.68%, reaching the highest results for polymer coating B and the lowest for composite coating D. However, composite coatings C and D presented a higher value of the τ parameter, suggesting that the presence of ceramics not only reduces the sorption capacity, but also slows down the penetration speed of the fluid inside the material.

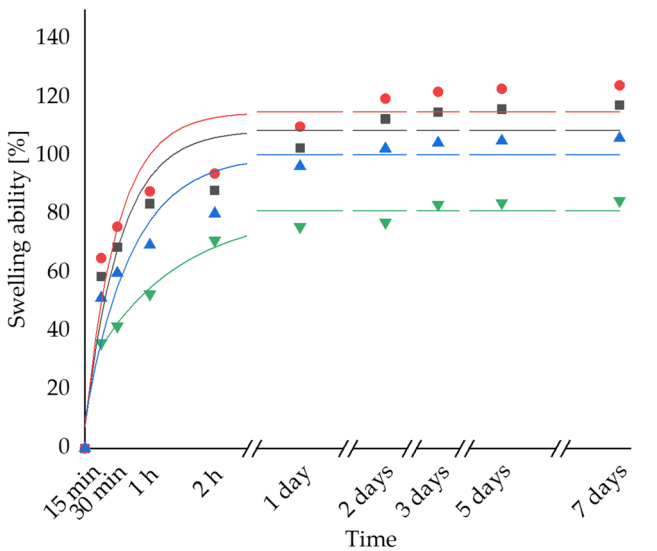

Fig. 2 Swelling kinetics of coatings A–D in PBS. The solid lines indicate fittings for the swelling ability of the individual samples.

Table 3 Rate parameter (τ) and equilibrium swelling (S_e) of the tested samples

Coating symbol	S_e [%]	τ
A	108.97 ± 4.68	32.72 ± 8.39
B	115.23 ± 5.10	30.06 ± 8.01
C	100.44 ± 4.35	43.24 ± 11.27
D	81.26 ± 1.63	79.15 ± 15.78

It is significant that even low sorption capacity and swelling of the material confirms the potential use of the biomaterial as a carrier of the active substance. It has been demonstrated that swelling of the material is one of the mechanisms of drug release, since during diffusion of liquid molecules into the interior of the material, molecules of the drug or other active substances are leached outward.[36,37] The results were the basis for modifying the coatings with clindamycin, and thus developing the carriers.

Potentiometric analysis was performed to determine the changes in the pH value of the PBS solution in which the coatings were incubated for 40 days (Fig. 3, top). This allowed to determine the stability of the materials under conditions simulating the environment of a living organism. Regardless of the composition and chemical formulation, the samples behaved relatively similarly, and the pH value oscillated between 7 and 7.5, which is safe for the organism. The subtle changes could be the result of leaching of residual polymers or ceramic particles from the interior of the materials. This phenomenon is confirmed by ionic conductivity measurements (Fig. 3, bottom). If the material was inert and did not interact with PBS, the conductivity value would remain relatively constant.[38] Changes in the range of 130–190 mS are indicative of ion exchange occurring between the sample and the fluid. In this case, slightly higher conductivity values were observed for materials with a higher proportion of the ceramic phase (coatings C and D). It is possible that individual, fine ceramic grains leached from the polymer matrix into the solution, which increased the conductivity. However, no noticeable degradation of the materials was observed.

Based on the coating compositions labelled A–D, drug loaded materials were prepared (samples 1–5) with the antibiotic bound to the ceramic and/or polymer phase. The carriers were immersed in 60 mL of PBS, into which clindamycin was released. Fig. 4 presents the percentage of the antibiotic released after 24 h. The initial hours of drug treatment are extremely important, as inhibition of bacterial growth occurs then, significantly affecting the further development of the disease. It was observed that after 1 day, the largest amounts of the drug were released from coating no. 1 and 2, *i.e.*, biomaterials based on polymers alone (without the ceramic phase), in which clindamycin was bound to PVP and PEG. The results were similar, at 35% and 36.8%, respectively. Smaller values were observed for the composite coatings. In coating 4, the

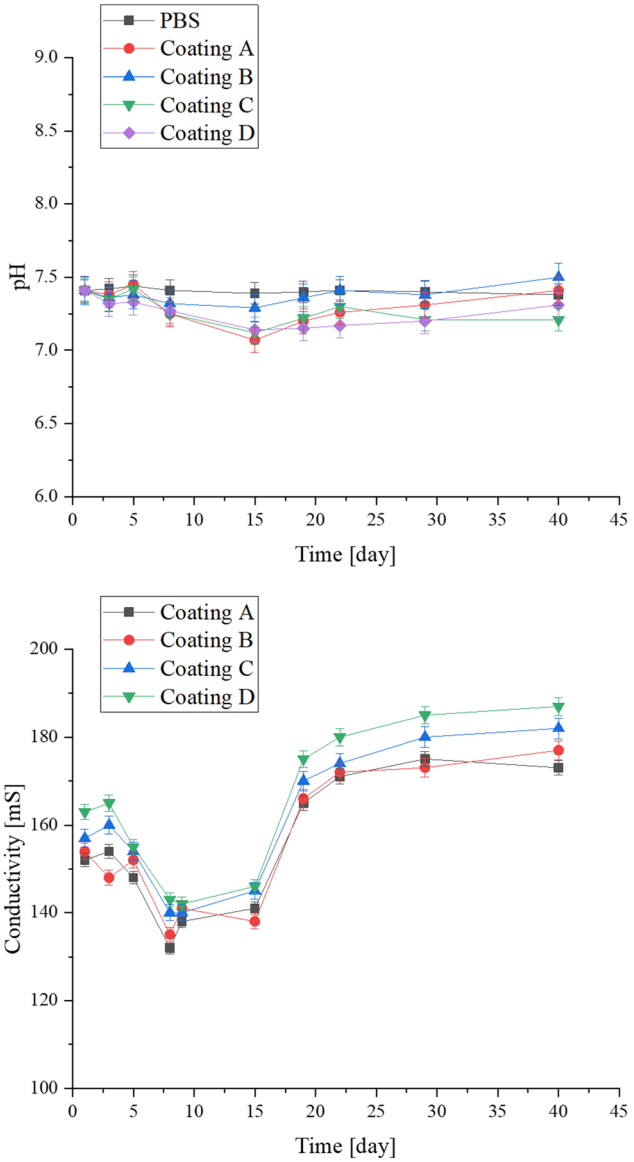

Fig. 3 Study of the behaviour of the coatings during a 40-day incubation in PBS; measured pH values (top) and ionic conductivity (bottom).

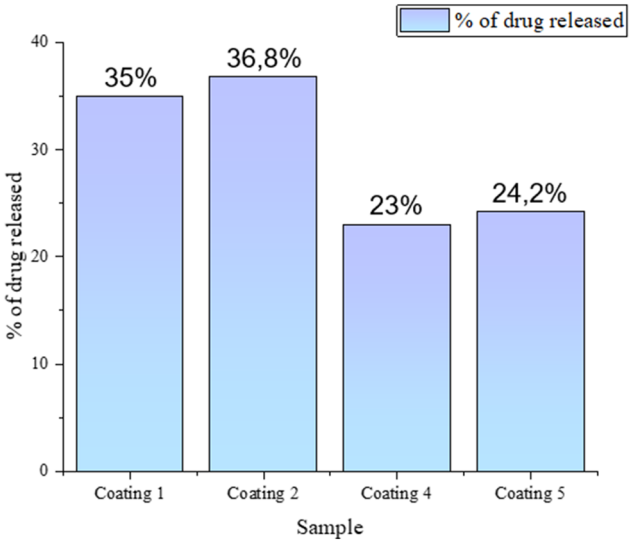

Fig. 4 Percentage of clindamycin released from coatings after 24 hours of incubation in PBS.

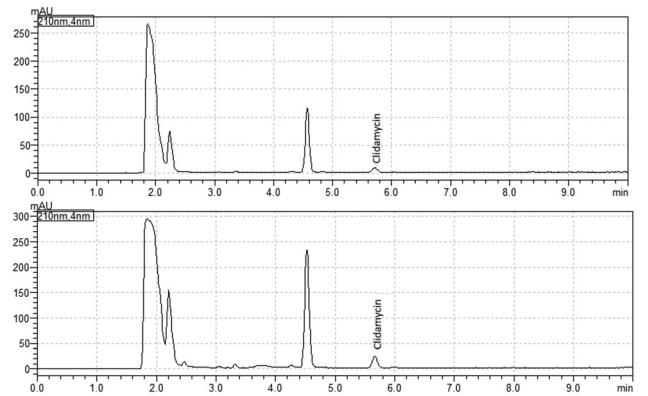

Fig. 5 Chromatograms of drug release from coating 5 after 1 day (top) and after 14 days (bottom).

drug was released from the polymer compound, and in sample 5, additionally from the interior of the drug-loaded HAp that was suspended in the matrix. However, the drug concentration values obtained were about one-third lower than those for the polymer materials at 23% and 24.2%, respectively.

The antibiotic release study was conducted for 14 days using HPLC. Fig. 5 presents chromatograms from days 1 and 14 of drug release from coating 5 into PBS and Fig. 6 presents a diagram demonstrating the amount of clindamycin in mg mL^{-1} released over time. Furthermore, the mechanism of release of the active ingredient from inside the swelling polymer matrix is presented schematically.

The trend observed as early as 24 hours continues until the end of the study, and the highest amount of drug escapes from coating 2 (PVP/PEG/COL). Finally, on the 14th day of measurement, it releases the largest amount of antibiotics, just over 25 mg, which is 83.6% of the total amount in the material. A slightly lower, although similar, value was observed for coating 1 (PVP/PEG) at 79.2%. As with the swelling results, composite materials exhibit the lowest values. Significantly, 71.6% of the drug was released from coating 4 and 72.6% from coating 5, while in the second one, clindamycin was bound to both the polymer and the ceramic phases. Such similar values suggest that the drug molecules are unable to escape from the hydroxyapatite grains and then pass through the polymer network. Presumably, this is the reason why it was not possible to determine the drug concentration for coating 3, containing clindamycin-modified hydroxyapatite, without the presence of the drug in the matrix.

Release rate studies confirm that all materials exhibit the nature of an active substance carrier. However, previous

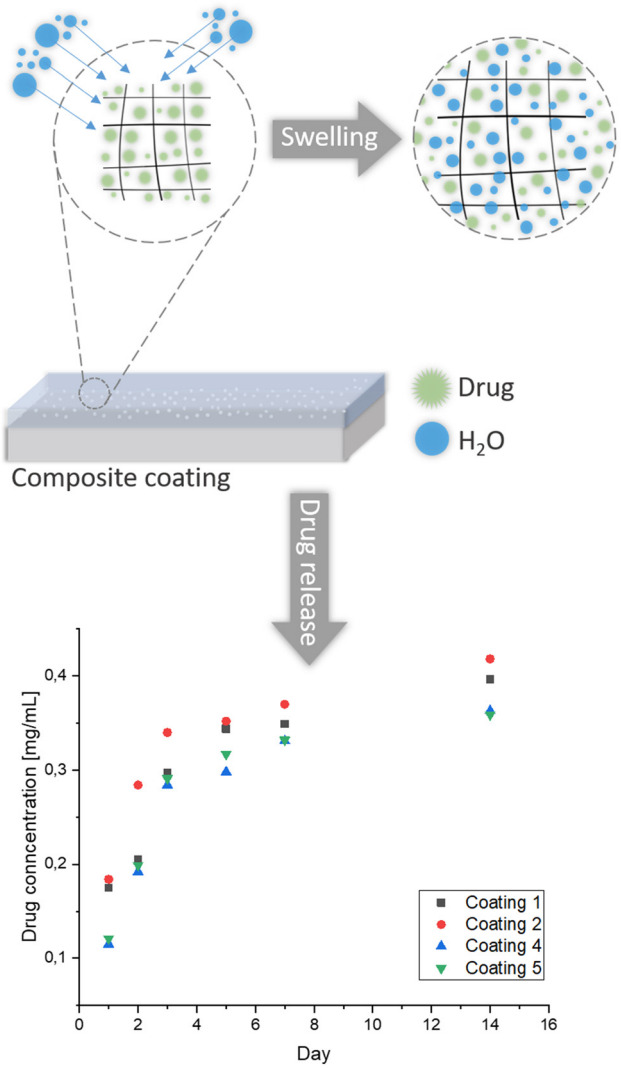

Fig. 6 Scheme of material swelling due to the penetration of aqueous solution and the rate of drug release from the polymer and composite coatings into PBS.

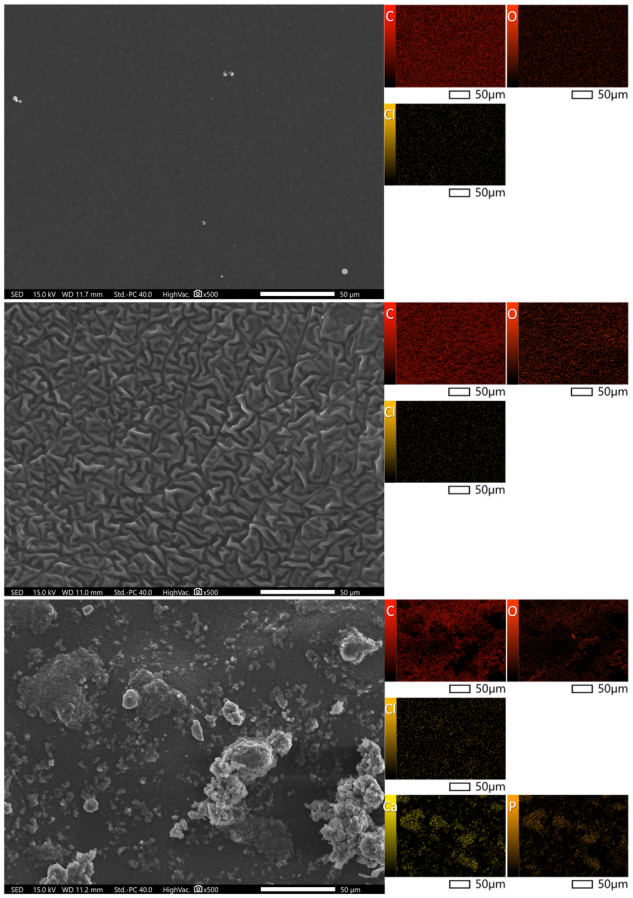

Fig. 7 Analysis of the morphology of clindamycin coatings before incubation for samples 1 (top), 2 (middle) and 4 (bottom) with mapping.

studies have suggested that in the context of bone tissue regeneration, the composite coating has the greatest potential in terms of physicochemical and tribological properties. Although polymer coatings 1 and 2 released more drug, the lack of hydroxyapatite caused them to lack bioactivity toward hard tissue regeneration. Clindamycin was determined to have a retention time of 5.7 minutes. An increase in the peak absorbance intensity with time could be observed. The other peaks detected earlier were presumably from the crosslinking agent or PVP and/or PEG polymers, as they appeared in each sample of both composite and polymer coatings. However, this requires further investigation. Considering the above results, drug release depends on time and the type of carrier as well as its composition.

The surface morphology of the obtained composite coatings before incubation in PBS solution is presented in Fig. 7. Analysing the SEM images, it can be seen that coatings 1 and 2 are characterized by a smooth surface, while EDS analysis (Table 4) confirms that carbon and oxygen are derived from the polymers. Moreover, analysis of the surface morphology of coating 4 demonstrates the presence of crystals in the polymer surface that correspond to the apatite layers, which confirm the occurrence of calcium and phosphorus in the EDS spectrum and elemental mapping.

In all three coatings, there exists clindamycin, which contains chlorine ions. Analysing the EDS spectra, it can be seen that this element is present in all the samples examined and is evenly distributed on each sample. Chlorine ions are not present in the chemical structure of any of the other components used in the development of the coating, hence it can be concluded that their presence confirms the modification with clindamycin, or more precisely clindamycin hydrochloride.

During the 14-day incubation in PBS solution, there were visible changes in the surface morphology of the obtained antibiotic composite coatings, as presented in Fig. 8. In both samples 1 and 2, characteristic crystals are visible, deposited on the polymer surface. In the EDS analysis (Table 5) and elemental mapping, ions from the composition of the incubation fluid appear. The presence of Na, Cl, K and Ca ions

Table 4 Elemental EDS analysis of coatings before the incubation period, and a summary of mass [%] and atomic [%] amounts of the individual elements

	Coating 1		Coating 2		Coating 4	
Element	Mass [%]	Atom [%]	Mass [%]	Atom [%]	Mass [%]	Atom [%]
C	65.26 ± 0.13	71.50 ± 0.14	63.93 ± 0.11	70.24 ± 0.12	57.21 ± 0.12	65.70 ± 0.14
O	34.59 ± 0.24	28.45 ± 0.20	36.06 ± 0.20	29.71 ± 0.17	37.45 ± 0.23	32.29 ± 0.20
Cl	0.15 ± 0.01	0.06 ± 0.00	0.12 ± 0.01	0.05 ± 0.00	0.06 ± 0.01	0.02 ± 0.00
Ca	—	—	—	—	3.61 ± 0.05	1.24 ± 0.02
P	—	—	—	—	1.66 ± 0.03	0.74 ± 0.01

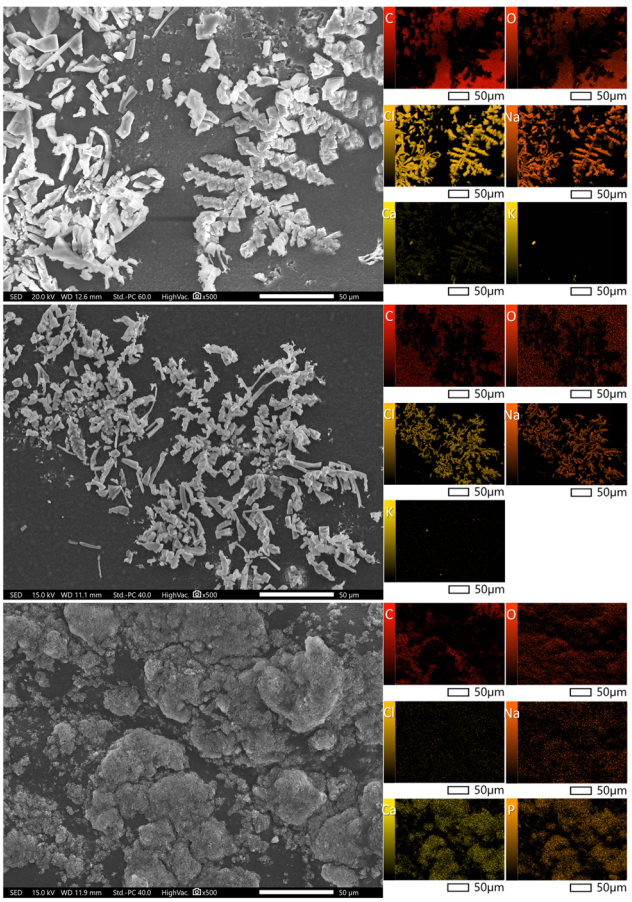

Fig. 8 Analysis of the morphology of clindamycin coatings after incubation in PBS for samples 1 (top), 2 (middle) and 4 (bottom) with mapping.

demonstrates that the biomaterial reacts with the solution in which it is incubated.

However, composition 4 exhibits the presence of ions from the incubation fluid. During the 14-day incubation period, there occurred changes visible on the surface of the obtained composite coatings of the active substance. Significant changes in the surface morphology as a result of incubation were observed for coating 4.

As a result of the interactions of bioactive hydroxyapatite with PBS, new apatite layers precipitated on the surface. This indicates the bioactivity of the coating towards apatite nucleation and suggests that not only can the coating serve as a drug carrier, but compared to the polymeric samples 1 and 2, it exhibits additional biological functions. Both changes in surface appearance and an increase in the amount of Ca and P elements during EDS microanalysis can be observed.

Clindamycin is widely used to treat bone infections caused by *Staphylococcus* due to its numerous advantages, including high bone penetration with long-lasting activity against bacterial biofilm formation and adhesion, high biodistribution, and low costs of synthesis and treatment.[39,40]

It was demonstrated that the obtained composites release clindamycin in biologically active and effective doses. The clindamycin-modified composite coatings 1, 3, 4, and 5 released the antibiotic, causing a statistically significant ($p < 0.001$) reduction in the metabolic activity of *S. aureus* ATCC 29213 to 2.3 ± 0.5%, 2.9 ± 1.4%, 2.2 ± 1.4%, and 2.7 ± 0.5%, respectively, compared to the untreated bacterial culture (Fig. 9). We have also shown that clindamycin-modified coatings do not differ with regard to their antimicrobial potential, which indicates a similar profile of the antibacterial properties of the tested com-

Table 5 Elemental EDS analysis of coatings after the incubation period in PBS, and a summary of mass [%] and atomic [%] amounts of the individual elements

	Coating 1		Coating 2		Coating 4	
Element	Mass [%]	Atom [%]	Mass [%]	Atom [%]	Mass [%]	Atom [%]
C	60.93 ± 0.17	72.96 ± 0.21	59.56 ± 0.14	70.79 ± 0.17	34.60 ± 0.12	47.17 ± 0.16
O	18.48 ± 0.15	16.62 ± 0.14	22.96 ± 0.15	20.49 ± 0.13	40.34 ± 0.23	41.29 ± 0.24
Na	9.47 ± 0.05	5.92 ± 0.03	7.73 ± 0.05	4.80 ± 0.03	0.99 ± 0.03	0.70 ± 0.02
Cl	10.80 ± 0.04	4.38 ± 0.02	9.46 ± 0.06	3.81 ± 0.02	0.36 ± 0.01	0.17 ± 0.01
K	0.21 ± 0.01	0.08 ± 0.00	0.20 ± 0.01	0.07 ± 0.00	0.27 ± 0.02	0.11 ± 0.01
Ca	0.10 ± 0.01	0.04 ± 0.00	0.09 ± 0.01	0.03 ± 0.00	15.34 ± 0.111	6.27 ± 0.04
P	—	—	—	—	8.11 ± 0.06	4.29 ± 0.03

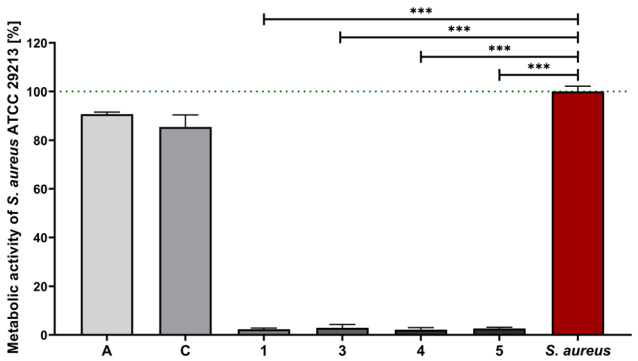

Fig. 9 Antibacterial activity of the clindamycin-modified composite coatings (1, 3, 4 and 5) and clindamycin-free references (A and C) against *S. aureus* ATCC 29213. The green line represents the reference metabolic activity of non-treated *S. aureus* (red bar). Results are shown as mean values with standard deviations (SD) of four independent experiments performed in triplicate for each experimental variant. Statistical significance – ***$p < 0.001$.

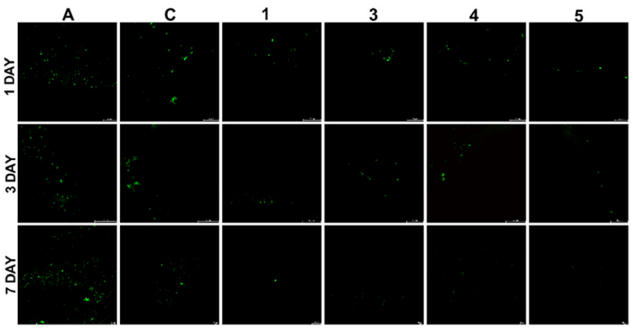

Fig. 10 Representative images of the biofilm formed by *S. aureus* on the clindamycin-modified coatings (1, 3, 4 and 5) or the control coatings (A and C) after 1, 3 or 7 days of incubation. Green fluorescence presents live bacteria on composites.

posites. Unlike coatings containing clindamycin, their reference samples (A and C) did not exhibit the ability to reduce the metabolic activity of bacteria.

A well-described technique for obtaining biodegradable composites with antibacterial properties is placing antibiotics in a ceramic phase, which is usually based on calcium sulfate or calcium phosphate. Local release of antibiotics from biodegradable and dissolving ceramic carriers increases the effectiveness of bacterial eradication after possible post-implantation infection and, therefore, results in better osseointegration of the biocomposite.[41,42] In this study, the suitability of composite coatings containing clindamycin in the ceramic or polymer phase and in both layers for eradicating *S. aureus* was demonstrated. It was revealed previously that clindamycin-loaded nanosized calcium phosphate powders have strong antistaphylococcal properties and can be considered as components of antibacterial biocomposites.[27]

S. aureus is one of the leading causes of post-implantation bone tissue infections associated with biofilm formation. The attachment of *S. aureus* to orthopaedic implants and host tissue, as well as the formation of a mature biofilm, plays an essential role in the persistence of chronic infections and the impairment of host bone regeneration mechanisms. Biofilm formation reduces susceptibility to antibacterial agents and immune system defence mechanisms, leading to a worsening prognosis of implant acceptance and the possibility of developing bacteremia.[43,44] A scanning confocal macroscope (SCM) was used to visually examine the anti-biofilm activities of clindamycin-modified coatings and clindamycin-free reference samples. To evaluate the biofilm inhibition properties, *S. aureus* ATCC 29213 was cultured with the coating samples for 1, 3, and 7 days and then observed using a SCM. As presented in Fig. 10, entirely green fluorescence of live bacteria was observed across the biofilm on the control coating groups (A and C). The presence of live bacteria throughout the experiment reached the highest degree of biofilm coverage of clindamycin-free coatings A and C after 7 days of culture with *S. aureus*. In the case of clindamycin-modified coatings (1, 3, 4 and 5), a low degree of biofilm development was observed after 1, 3 and 7 days of incubation with bacteria, resulting from the antibacterial effect of clindamycin released from the composites. The results show that adding clindamycin effectively limits biofilm formation on the first day of incubation, regardless of whether the drug is bound to the polymer or ceramic phase of the composite.

Biomaterials used in regenerative medicine must have appropriate mechanical and physicochemical properties supporting the regeneration of damaged tissues, but apart from them, one of the most important parameters they should meet is their biocompatibility and lack of cytotoxicity.[45] To address this aspect, we assessed the impact of coating C and coating 4 (sample C modified with clindamycin in the polymer matrix) on the metabolic activity of two cell lines, L929 and hFOB 1.19. These samples were selected because compared to polymer coatings, they not only served as a drug carrier, but also exhibited bioactivity toward the formation of new apatite layers during incubation in PBS. It was demonstrated that the obtained coatings remained cytocompatible for both tested cell lines. The cell viability of L929 fibroblasts remained over 90% (sample C: 91.3% ± 11.5% and sample 4: 92.7% ± 6.9%) and the presence of materials had no significant effect on cell viability compared to either the positive control (102.1% ± 4.2%) or the reference material (95.8% ± 11.8%). Similarly, none of the tested materials (coating C: 98.9% ± 17.0% and coating 4: 88.7% ± 9.8%) significantly affected the cell metabolic activity compared to the reference material (103.6% ± 4.2%) for the hFOB 1.19 cell line (Fig. 11). In both L929 and hFOB 1.19 cell lines after incubation with the tested coatings, cell viability remained over 70%, which met the ISO-10993-5-2009 criteria and proved their cytocompatibility. The presented results confirm the *in vitro* safety of the tested materials and their potential application in *in vivo* studies, in particular those aimed at bone tissue regeneration, due to their cytocompatibility with the human osteoblast cell line.

The current study's results confirm that the clindamycin-modified coatings do not cause changes in L929 cell metabolic

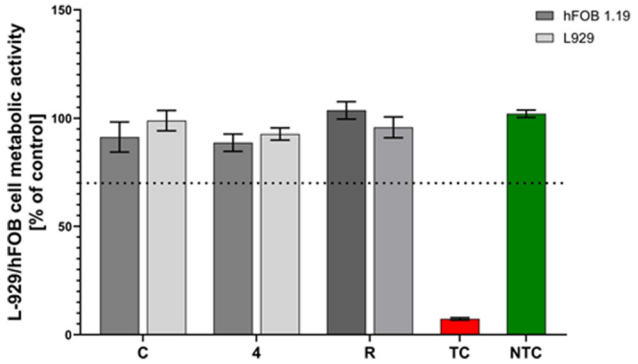

Fig. 11 The metabolic activity of mouse L929 fibroblasts and human hFOB 1.19 fetal osteoblasts after 24 h of incubation with coatings. NTC – non-treated control (green bar) and TC – treated control (red bar), in terms of cell metabolic activity; R – biomaterials derived from a medically certified peripheral venous catheter. Dotted line – 70% of the cell viability cutoff. The data are presented as mean ± SD for the three separate experiments.

activity, making them cytocompatible. The research also includes a human osteoblast cell model, confirming the safety of the composite coatings tested against hFOB 1.19 cells. These promising results indicate the potential use of the coatings for bone tissue regeneration.

The results presented in Fig. 12A indicate the lack of potentially harmful effects of the tested biomaterials in the *in vivo* system. Observation of the biomaterials' implantation sites demonstrates no local inflammatory reaction, and the healing of surgical wounds does not display any signs of inflammation. Measurement of the concentrations of pro-inflammatory cytokines (IL-1β and TNF-α) confirms the absence of a systemic inflammatory response to the implanted biomaterials. The results are then compared to the levels of cytokines found in the sera of the control animals (Fig. 12B and D). Although the concentrations of both pro-inflammatory cytokines are higher 7 days after biomaterial implantation compared to 30 days, this is related to the body's mobilisation immediately after the surgical procedure.

Measurement of the anti-inflammatory cytokine IL-10 in the animal sera indicated higher levels 30 days after the implantation of biomaterials, particularly those not modified with clindamycin (C). Elevated levels of IL-10 in the animal sera 30 days after surgery correlated in some way with the low levels of pro-inflammatory cytokines in the same samples (Fig. 12C).

Our findings align with those of Rodriguez *et al.*,[46] who observed a decrease in the levels of pro-inflammatory cytokines IL-1β and TNF-α over time (up to 14 days), following the surgical implantation of biomaterials in a rat model. Moreover, they observed that levels of anti-inflammatory cytokines, such as IL-10 and TGFβ, increased across all study groups from day 4 to day 14. Levels of anti-inflammatory cytokines are expected to rise over time as the wound healing process progresses.[47]

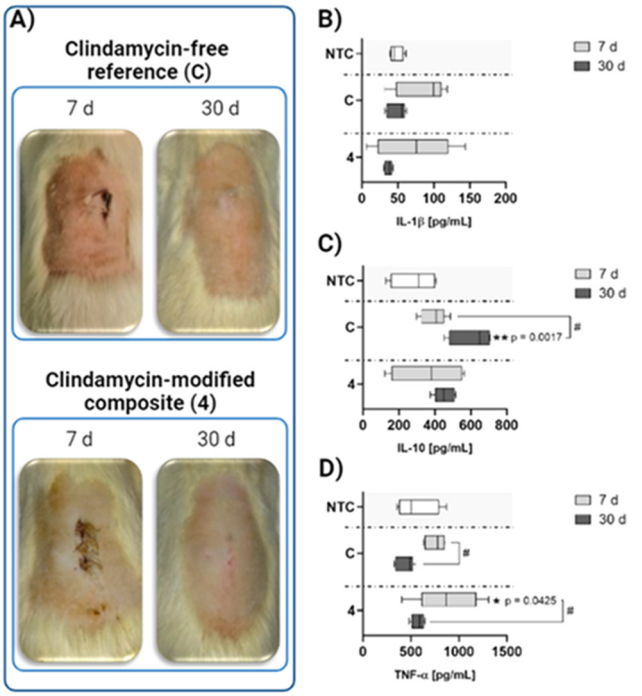

Fig. 12 Representative images demonstrating the implantation sites for biomaterials: clindamycin-free references (C) (top panel) and clindamycin-modified composite (4) at 7 and 30 days after implantation (A). The concentration of interleukin-1 beta – IL-1β (B), interleukin 10 – IL-10 (C), and tumor necrosis factor α – TNF-α (D) in the serum samples obtained from the animals at 7 and 30 days after implantation. NTC – non-treated control (rats not subjected to implantation of the biomaterials). Number of animals, n = 3. * – Statistical significance *vs.* the NTC within the time point; the p-value is given after the asterisk. # – Statistical significance ($p < 0.05$) with regard to the time points within the group. Data are presented as minimum and maximum values represented as a line.

Conclusions

Hybrid polymer–ceramic composite coatings have been successfully developed for the controlled release of clindamycin. The developed method of synthesis under UV light, based on a photocrosslinking procedure, enabled continuous, fully crosslinked materials without ripples or irregularities to be obtained. The coatings exhibited a lower sorption capacity as the proportion of the ceramic phase increased. Related to this phenomenon is the release of the drug, which was greater for polymeric materials without hydroxyapatite. It was also demonstrated that the coating containing the drug bound to hydroxyapatite was not able to release it in satisfactory amounts. The largest amount of clindamycin was released from the coating exhibiting the best sorption capacity. Elemental EDS analysis confirmed the presence of chlorine ions derived from the antibiotic in the material before the immersion period in PBS, and the surface morphology indicated changes in the structure after the incubation period. The *in vitro* release of clindamycin from the coatings indicated its role in developing a controlled drug delivery system. Antimicrobial properties were confirmed for all materials

against *S. aureus*. The conducted studies had a preliminary character as well as were aimed to select materials for further procedures under *in vivo* conditions. Evaluation of the local tissue response and systemic response to the *in vivo* implantation of the coatings indicates that there are no potentially harmful effects of the developed biomaterials. However, further research is required to fully determine the application potential of the hybrid polymer/ceramic composite coatings presented in this manuscript.

Author contributions

Conceptualization, D.S.; methodology, D.S. and M.M.U.; software, D.S.; validation, D.S.; formal analysis, D.S., K.N. and M. M.U.; investigation, D.S., M.M.U., W.F. and A.T.; resources, D. S.; data curation, D.S.; writing—original draft preparation, D. S., K.N. M.M.U. and A.T.; writing—review and editing, A.S.-K.; visualization, D.S.; supervision, A.S.-K.; project administration, A.S.-K.; funding acquisition, A.S.-K. and M.M.U.; planning, execution, and analysis of the *in vivo* experiments, A.S.-G., M. W., and A.K. All authors have read and agreed to the published version of the manuscript.

Ethical statement

All animal procedures were performed in accordance with the Guidelines for Care and Use of Laboratory Animals of the University of Lodz and approved by the Local Ethical Committee for Animal Experiments based at the Medical University of Lodz (Protocol No. ŁB192/2021 dated February 8, 2021).

Data availability

Data for this article, including SEM imaging, EDS microanalysis, HPLC drug release determination and incubation results, are available at the Mendeley Data repository at **https://doi.org/10.17632/jytvts9z3t.1**. Data for this article including the biosafety assessment against L929 cells, antimicrobial properties and *in vivo* evaluation are available at **https://hdl.handle.net/11089/52948**.

Conflicts of interest

There are no conflicts to declare.

Acknowledgements

The "Multifunctional biologically active composites for applications in bone regenerative medicine" project was carried out within the TEAM-NET program of the Foundation for Polish Science, financed by the European Union under the European Regional Development Fund (grant number POIR.04.04.00-00-16D7/18). The authors gratefully acknowledge the financial support.

The authors express their thanks to Karolina Rudnicka and Przemysław Płociński from the Department of Immunology and Infectious Biology, Faculty of Biology and Environmental Protection, University of Lodz, for their help with the experimental design, data analysis, and supervision. The authors would like to express their gratitude to Sylwia Michlewska and Marika Grodzicka from the Laboratory of Microscopic Imaging and Specialized Biological Techniques, Faculty of Biology and Environmental Protection, University of Lodz, for their help in visualising bacterial biofilms.

References

1 D. Arcos, A. R. Boccaccini, M. Bohner, A. Díez-Pérez, M. Epple, E. Gómez-Barrena, A. Herrera, J. A. Planell, L. Rodríguez-Mañas and M. Vallet-Regí, *Acta Biomater.*, 2014, **10**, 1793–1805.
2 C. Joe, Top Companies in Bio-Composites Market by Size, Share, Historical and Future Data & CAGR | Report by Vantage Market Research, 2023.
3 A. L. Jardini, M. A. Larosa, R. M. Filho, C. A. D. C. Zavaglia, L. F. Bernardes, C. S. Lambert, D. R. Calderoni and P. Kharmandayan, *J. Cranio-Maxillofac. Surg.*, 2014, **42**, 1877–1884.
4 S. B. Naique, M. Pearse and J. Nanchahal, *J. Bone Jt. Surg. – Ser. B*, 2006, **88**, 351–357.
5 M. Djošić, A. Janković and V. Mišković-Stanković, *Materials*, 2021, **14**, 5391.
6 Y. Zhang, Y. Xu, H. Kong, J. Zhang, H. F. Chan, J. Wang, D. Shao, Y. Tao and M. Li, *Exploration*, 2023, **3**, 20210170.
7 W. Kolasiński, *Pol. J. Surg.*, 2018, **90**, 1–7.
8 J. Parvizi, S. Barnes, N. Shohat and C. E. Edmiston, *Am. J. Infect. Control*, 2017, **45**, 1267–1272.
9 X. Lu, R. Chen, J. Lv, W. Xu, H. Chen, Z. Ma, S. Huang, S. Li, H. Liu, J. Hu and L. Nie, *Acta Biomater.*, 2019, **99**, 363–372.
10 E. A. Masters, R. P. Trombetta, K. L. de Mesy Bentley, B. F. Boyce, A. L. Gill, S. R. Gill, K. Nishitani, M. Ishikawa, Y. Morita, H. Ito, S. N. Bello-Irizarry, M. Ninomiya, J. D. Brodell, C. C. Lee, S. P. Hao, I. Oh, C. Xie, H. A. Awad, J. L. Daiss, J. R. Owen, S. L. Kates, E. M. Schwarz and G. Muthukrishnan, *Bone Res.*, 2019, **7**(1), 20.
11 WHO, World Health Organization.
12 M. B. Browning, S. N. Cereceres, P. T. Luong and E. M. Cosgriff-Hernandez, *J. Biomed. Mater. Res., Part A*, 2014, **102**, 4244–4251.
13 Z. Peng, C. Ji, Y. Zhou, T. Zhao and R. M. Leblanc, *Appl. Mater. Today*, 2020, **20**, 100677.
14 A. Kuźmińska, B. A. Butruk-Raszeja, A. Stefanowska and T. Ciach, *Colloids Surf., B*, 2020, **192**, 4–9.

15 M. S. B. Husain, A. Gupta, B. Y. Alashwal and S. Sharma, *Energy Sources, Part A*, 2018, **40**, 2388–2393.
16 E. E. Doğan, P. Tokcan, M. E. Diken, B. Yilmaz, B. K. Kizilduman and P. Sabaz, *Adv. Mater. Sci.*, 2019, **19**, 32–45.
17 P. Franco and I. De Marco, *Polymers*, 2020, **12**, 18–21.
18 L. Yu, D. W. Rowe, I. P. Perera, J. Zhang, S. L. Suib, X. Xin and M. Wei, *ACS Appl. Mater. Interfaces*, 2020, **12**, 18235–18249.
19 L. Sbricoli, R. Guazzo, M. Annunziata, L. Gobbato, E. Bressan and L. Nastri, *Materials*, 2020, **13**, 1–16.
20 A. Terzi, N. Gallo, S. Bettini, T. Sibillano, D. Altamura, M. Madaghiele, L. De Caro, L. Valli, L. Salvatore, A. Sannino and C. Giannini, *Macromol. Biosci.*, 2020, **20**, 1–18.
21 L. Ruiz-Rodriguez, P. Loche, L. T. Hansen, R. R. Netz, P. Fratzl, E. Schneck, K. G. Blank and L. Bertinetti, *MRS Bull.*, 2021, **46**, 889–901.
22 A. Sionkowska, K. Adamiak, K. Musiał and M. Gadomska, *Materials*, 2020, **13**, 4217.
23 M. Diotallevi, P. Checconi, A. T. Palamara, I. Celestino, L. Coppo, A. Holmgren, K. Abbas, F. Peyrot, M. Mengozzi and P. Ghezzi, *Front. Immunol.*, 2017, **8**, 1239.
24 C. Gaucher, A. Boudier, J. Bonetti, I. Clarot, P. Leroy and M. Parent, *Antioxidants*, 2018, **7**(5), 62.
25 L. Wang, M. Shen, Q. Hou, Z. Wu, J. Xu and L. Wang, *Int. J. Biol. Macromol.*, 2022, **222**, 1175–1191.
26 A. M. Tomala, D. Słota, W. Florkiewicz, K. Piętak, M. Dyląg and A. Sobczak-Kupiec, *Lubricants*, 2022, **10**, 58.
27 D. Słota, K. Piętak, W. Florkiewicz, J. Jampílek, A. Tomala, M. M. Urbaniak, A. Tomaszewska, K. Rudnicka and A. Sobczak-Kupiec, *Nanomaterials*, 2023, **13**(9), 1469.
28 K. Kabiri, H. Omidian, S. A. Hashemi and M. J. Zohuriaan-Mehr, *Eur. Polym. J.*, 2003, **39**, 1341–1348.
29 X. Gong, Z. Liang, Y. Yang, H. Liu, J. Ji and Y. Fan, *Regener. Biomater.*, 2020, **7**, 271–281.
30 European Committee on Antimicrobial Susceptibility Testing. Breakpoint Tables for Interpretation of MICs and Zone Diameters, Version 13.0: European Committee on Antimicrobial Susceptibility Testing, Växjö, Sweden, 2013.
31 M. Biernat, A. Szwed-Georgiou, K. Rudnicka, P. Płociński, J. Pagacz, P. Tymowicz-Grzyb, A. Woźniak, M. Włodarczyk, M. M. Urbaniak, A. Krupa, P. Rusek-Wala, N. Karska and S. Rodziewicz-Motowidło, *Int. J. Mol. Sci.*, 2022, **23**(22), 14315.
32 K. Nawrotek, M. Tylman, K. Rudnicka, J. Gatkowska and M. Wieczorek, *Carbohydr. Polym.*, 2016, **152**, 119–128.
33 P. Piszko, M. Włodarczyk, S. Zielińska, M. Gazińska, P. Płociński, K. Rudnicka, A. Szwed, A. Krupa, M. Grzymajło, A. Sobczak-Kupiec, D. Słota, M. Kobielarz, M. Wojtków and K. Szustakiewicz, *Int. J. Mol. Sci.*, 2021, **22**(16), 8587.
34 H. Susi, J. S. Ard and R. J. Carroll, *Biopolymers*, 1971, **10**, 1597–1604.
35 E. Karna, L. Szoka, T. Y. L. Huynh and J. A. Palka, *Cell. Mol. Life Sci.*, 2020, **77**, 1911–1918.
36 A. Martinac, J. Filipović-Grčić, B. Perissutti, D. Voinovich and Ž. Pavelić, *J. Microencapsulation*, 2005, **22**, 549–561.
37 G. Leyva-Gómez, M. L. Del Prado-Audelo, S. Ortega-Peña, N. Mendoza-Muñoz, Z. Urbán-Morlán, M. González-Torres, M. G. Del Carmen, G. Figueroa-González, O. D. Reyes-Hernández and H. Cortés, *Pharmaceutics*, 2019, **11**(5), 217.
38 A. Kaczmarek-Pawelska, K. Winiarczyk and J. Mazurek, *J. Achiev. Mater. Manuf. Eng.*, 2017, **81**, 35–40.
39 M. Bustamante-Torres, B. Arcentales-Vera, J. Estrella-Nuñez, H. Yánez-Vega and E. Bucio, *Macromol*, 2022, **2**, 258–283.
40 B. Agathe, V.-G. Véronique, L. Delphine, B. Odile, B. Morgane, H. Maxime, O. Xavier, D. Saidou and B.-S. Firouzé, *Diagn. Microbiol. Infect. Dis.*, 2021, **99**, 115225.
41 J. Ferguson, M. Diefenbeck and M. Mcnally, *J. Bone Jt. Infect.*, 2017, **2**, 38–51.
42 V. Kavarthapu, J. Giddie, V. Kommalapati, J. Casey, M. Bates and P. Vas, *J. Clin. Med.*, 2023, **12**(9), 3239.
43 J. L. Lister and A. R. Horswill, *Front. Cell. Infect. Microbiol.*, 2014, **4**, 1–9.
44 M. Bhattacharya, D. J. Wozniak, P. Stoodley and L. Hall-Stoodley, *Expert Rev. Anti-Infect. Ther.*, 2015, **13**, 1499–1516.
45 M. Sokolsky-Papkov, K. Agashi, A. Olaye, K. Shakesheff and A. J. Domb, *Adv. Drug Delivery Rev.*, 2007, **59**, 187–206.
46 A. Rodriguez, H. Meyerson and J. M. Anderson, *J. Biomed. Mater. Res., Part A*, 2009, **89**, 152–159.
47 K. L. Singampalli, S. Balaji, X. Wang, U. M. Parikh, A. Kaul, J. Gilley, R. K. Birla, P. L. Bollyky and S. G. Keswani, *Front. Cell Dev. Biol.*, 2020, **8**, 636.